Mean Field Analysis of the SU(3) Lattice Gauge System Coupled with a Scalar Field

Toshinobu MAEHARA

Department of Physics, Hiroshima University,
Higashi-senda-machi, Naka-ku, Hiroshima 730

(J. Sci. Hiroshima Univ., Ser. A, Vol.49, (1985), No.3)

Abstract

We investigate the phase structure of the SU(3) lattice gauge system coupled with a scalar field on the basis of the lowest-order mean field approximation. Two cases are considered for the SU(3) representation of the scalar field. For the fundamental representation, the resultant phase diagram is shown to agree qualitatively with the Monte Carlo results, if we take into account the analyses made in the limiting cases for the parameters of the system. For the adjoint one, however, the transition caused by the gauge fields of the residual subgroup SU(2)×U(1) does not appear due to the too simple form we assume for the mean gauge-field.

§1. Introduction

Gauge model has a variety of phases according to the values of its characteristic constants such as a gauge coupling and masses of fundamental fermions. In the quantum chromodynamics the confined phase is smoothly connected to the asymptotically free phase and no phase transition (at least up to second order) is expected.[1] The single phase structure assures that quarks are never liberated but behave as if they were free in hadrons at a short distance. When the system is held in the thermal equilibrium with a finite temperature, however, the situation changes. Theoretical considerations[2] and the investigations using Monte Carlo simulations (MCS)[3] have pointed out the possibility that a first-order deconfining transition exists at some critical temperature. If it is the case, we will find a quark-gluon phase in high-energy heavy-ion collisions and a new interesting physics will emerge. Phase transitions play an important role also in the grand unified theories. Since the symmetry assumed in such theories is not the one observed at low energies, we have to break it by introducing scalar fields. The symmetry is kept unbroken at high temperatures. After the system is cooled down below a critical temperature the vacuum turns to be false and makes a transition to the true one with a broken symmetry. This transition gives a hint for the interpretation of the flatness and the homogeneity of the universe in the inflationary senario.[4] Parameters in the potential for the scalar fields should be chosen so that the system shows a desired breaking pattern at low energies. Thus it is very interesting to study phase structures of various gauge models.

In this report we discuss the SU(3) lattice gauge system coupled with a scalar field. Recently the author has investigated the model using computer simulations in collaboration with some members of his laboratory.[5,6] In the case that the scalar field belongs to the fundamental representation, they have found that the two-parameter phase-plane is governed by a single phase although a transition line lies in the weak coupling region. They have also studied the case of the scalar field in the adjoint representation. According to their result it is seen that even such a simple model gives rise to the quite complicated phase structure. In particular, they have found that the line of the transition of a Heisenberg spin system existing at a weak coupling limit extends to a cross-over region and is connected to that of an Ising-like transition at a strong coupling limit.

The Monte Carlo simulation may be the most powerful method to study the phase structure, but a full analysis of the system requires too long a CPU time. In practice, although the above authors have used a rather small lattice (3^4 or $6^3\times3$), more iterations are needed to determine the precise location and the order of critical structures. The present author has realized a necessity of theoretical analyses based on the other methods.

This situation was the main motivation of the present work. Thus it should be considered as a supplementary part to the previous Monte Carlo simulations.

The method used here is the mean field approximation (MFA). It can predict a gross structure of the phase, though it often leads to erroneous predictions on the order and/or the location of transition. Brezin and Drouffe have reformulated it in a way that the approximation may be improved by adding correction terms order by order.[7] For lattice gauge-higgs systems with a gauge group U(1), Pendleton has shown that results of the lowest-order MFA agree qualitatively with Monte Carlo data.[8] We extend his analysis to the case of the group SU(3). In order to compare our result with MCS, the scalar field is assumed to belong to the fundamental or the adjoint representation of SU(3).

In the next section, we explain the model in a rather detailed manner and review the results of the Monte Carlo analyses in this model. In §3 we apply the mean field approximation to the cases of the scalar fields belonging to the fundamental and adjoint representations respectively and we derive the self-consistency equations in the mean field approximation. The numerical solutions are given in §4. In §5 we discuss the phase structure of the system based on the numerical results. The final section is devoted to concluding remarks.

§2. SU(3) lattice gauge system coupled with a scalar field

We consider the SU(3) gauge-higgs system on a four-dimensional euclidean lattice. A gauge variable $U_{s\hat{\mu}}^{ij}$ is assigned to each link $(s,s+\hat{\mu}a)$ where s denotes a site, and $\hat{\mu}$ a unit vector pointing the positive direction of x_μ. The lattice spacing a is taken to be unity in the followings. Superscripts i and j run over the indices of the fundamental representation of SU(3), i.e., 1 to 3. A scalar field ϕ_s^i (ϕ_s^a) is defined on each site s and it is assumed to belong to the fundamental (adjoint) representation. The action of the whole system is a sum of a gauge and a scalar part:

$$S = S_U + S_\phi \ . \qquad (2.1)$$

We take the Wilson action for the gauge part

$$S_U = \beta\sum_p[1-\frac{1}{3}\mathrm{ReTr}(U_p)] \ , \qquad (2.2)$$

where U_p is an ordered product of $U_{s\hat{\mu}}$ along a plaquette, $\beta=6/g^2$ (g is a gauge coupling constant) and the summation is taken over the whole plaquettes. On the scalar field we impose a fixed norm condition

$$\sum_i|\phi_s^i|^2 = 1 \qquad \text{(fundamental repr.)} \qquad (2.3a)$$

or

$$\Sigma(\phi_s^a)^2 = 1 \quad \text{(adjoint repr.)} , \tag{2.3b}$$

for convenience. Then a naive discretisation of the minimally coupled Lagrangian gives

$$S_\phi^F = \gamma \sum_{s,\hat{\mu}} [1-\mathrm{Re}(\phi^\dagger_{s+\hat{\mu}} U_{s\hat{\mu}} \phi_s)] \tag{2.4a}$$

or

$$S_\phi^A = \gamma \sum_{s,\hat{\mu}} [1-\mathrm{Tr}(\Phi_{s+\hat{\mu}} U_{s\hat{\mu}} \Phi_s U^\dagger_{s\hat{\mu}})] , \tag{2.4b}$$

where superscripts F and A denote the fundamental and the adjoint representation, respectively. Here in the case of the adjoint representation, $\Phi_s=\Phi_s^\dagger$ is a matrix form $\Phi_s=\Sigma_a\phi_s^a\lambda^a/\sqrt{2}$, where λ^a_{ij} (a=1,...,8) is a Gell-Mann matrix. The parameter γ is proportional to the vacuum expectation value squared of the scalar field in the continuum limit. The partition function is defined as

$$Z = \int (dU)(d\phi)\ e^{-S} . \tag{2.5}$$

Functional integration measures are

$$(dU) = N_U^{-1} \prod_{s,\hat{\mu}} d^{18}U^{ij}_{s\hat{\mu}}\ \delta(U^{\dagger}U-1)\ \delta(\det U-1) \tag{2.6}$$

$$(d\phi)_F = N_F^{-1} \prod_{s} d^6\phi^i_s\ \delta(|\phi|^2-1) \tag{2.7a}$$

$$(d\phi)_A = N_A^{-1} \prod_{s} d^8\phi^a_s\ \delta(\phi^2-1)\quad , \tag{2.7b}$$

where N_U, N_F and N_A are normalisation constants. Various gauge fixing conditions can be imposed and then the MFA will give a different result.[8] It is suspected that the difference may be explained by taking into account higher-order corrections. It is, however, beyond the scope of this report to pursue this problem any further. Here we adopt the model without a gauge fixing. A state of the system is determined by minimizing a free energy density $F= -(\ell nZ)/\text{volume}$.

Let us comment on behaviours of the system in the extreme cases. The detailed discussions have been given elsewhere.[5,6]

(i) $\gamma=0$

The system reduces to an SU(3) pure gauge one. As mentioned in the previous section, it has no phase transition at a zero temperature although it is expected to have a first-order critical point at a finite temperature.

(ii) $\gamma=\infty$

It is the limit of an infinite vacuum expectation value of the scalar field. In the case of the triplet scalar field, the system is nothing but an SU(2) pure gauge one with an inverse temperature scaled by a factor 2/3, i.e. $2\beta/3$. The phase structure is similar to that of the SU(3) case except that the deconfining transition of the finite temperature is of the second order.

In the case of the octet scalar field, there are two possible residual symmetries, SU(2)×U(1) and U(1)×U(1). In Ref.6 it has been conjectured and confirmed by MCS that the former is the real residual symmetry. Two subsystems with symmetry SU(2) and with U(1) have their own critical natures independently. Then two critical points exist, corresponding to the finite-temperature deconfining transition of the SU(2) pure gauge system and the U(1)-deconfining transition. The latter occurs at a smaller value of β.

(iii) $\beta=0$

In this limit, the partition function of the system with a triplet scalar field is written as an analytic function of γ, since it factorizes, in the unitary gauge, into the product of integrals of gauge variables. For the system with an octet scalar field, no factorization occurs, but the system is described by a variable $D_s=\det(\Phi_s)$ if we perform integrations over gauge variables. The small γ expansion gives an effective action for D_s similar to that of the Ising system and predicts a transition at around $\gamma=5$.

(iv) $\beta=\infty$

In this limit both the fundamental and the adjoint scalar system become a four-dimensional Heisenberg spin system with a symmetry of O(6) and O(8), respectively. It is known that the Heisenberg-spin system has a second-order critical point in four dimensions. The critical point is estimated by applying an infra-red bound[10] for O(N) system

$$\gamma_c \geq \frac{N}{2} \int_0^\infty ds[\exp(-s)\cdot I_0(s)]^4 \quad , \tag{2.8}$$

where I_0 is a modified Bessel function of the zeroth order.

The analyses using Monte Carlo simulations have given phase diagrams shown in Fig.1. The O(6)-Heisenberg-spin transition starting at $(\beta,\gamma)\simeq(\infty,1)$ extends to the crossover region and terminates around $(\beta,\gamma)=(5,1)$ in Fig.1(a). It is consistent with the above study of the limiting cases. There is no critical point to which the line is connected. Because there is no critical point to which the line is connected, it must terminate before reaching the strong coupling limit. The end point lies in the crossover region, since the orderedness of spins loses its meaning in the disorder region of the gauge system. The dotted line is a critical-like structure connecting the crossover points of the SU(3, (β=0 limit) and SU(2) ($\beta=\infty$ limit) pure gauge system. This structure may be due to a size effect arising from smallness of the lattice. The phase diagram (Fig.1(b)) of the adjoint-scalar system is drawn for the finite-temperature case. The phase plane is divided into five parts by critical lines. Region

I and II are SU(3)-symmetric phases, where the former is the confined phase and the latter the deconfined. The broken phase consists of three parts, the SU(2)×U(1)-confined, the SU(2)-confined but U(1)-deconfined, and the fully deconfined one. The location of the Ising-like transition line in the strong coupling region is obscure owing to the rather small number of iterations. The phase diagram at a zero temperature is obtained by removing the finite temperature transition line from Fig.1(b). In order to verify these phase structures, we study the system based on the mean field method.

§3. Mean field approximation

The mean field approximation can be considered as a saddle point estimation of the partition function, where the variables are replaced by a new set of unconstrained variables. Self-consistency equations are, therefore, derived as a stationary condition for the effective action. Let us derive them for the SU(3) lattice gauge-higgs system in the case that the scalar field belongs to the fundamental representation. For the case of the adjoint representation, we will note the difference and give resultant formulae at the end of the section.

The unconstrained fields are introduced by inserting a unity into the integral of the partition function (2.5). For gauge variables, it reads

$$1 = \int_{-\infty}^{\infty} d^{18}V \ \delta(V-U)$$

$$= \int_{-\infty}^{\infty} d^{18}V \int_{-i\infty}^{i\infty} d^{18}M \ \exp\{-\mathrm{ReTr}[M^{\dagger}(V-U)]\} \quad , \qquad (3.1)$$

where we have dropped suffices s, $\hat{\mu}$ and superfices i, j. For the scalar fields we have

$$1 = \int_{\infty}^{\infty} d^{6}\eta \ \delta(\eta-\phi)$$

$$= \int_{-\infty}^{\infty} d^{6}\eta \int_{-i\infty}^{i\infty} d^{6}\xi \ \exp\{-\mathrm{Re}[\xi^{\dagger}(\eta-\phi)]\} \quad . \qquad (3.2)$$

The partition function is rewritten as

$$Z = \int (dU)(d\phi)\ \exp\{-S(U,\phi)\} \quad ,$$

$$= \int dV d\eta (dU)(d\phi)\ \delta(V-U)\delta(\eta-\phi)\ \exp\{-S(V,\eta)\} \quad ,$$

$$= \int dV dM d\eta d\xi (dU)(d\phi) \times\exp\{-S(V,\eta)-\mathrm{ReTr}[M^{\dagger}(V-U)]-\mathrm{Re}[\xi^{\dagger}(\eta-\phi)]\} \ . \quad (3.3)$$

If we perform the integration over the original variables in such a way as

$$e^{W(M)} = \int (dU)\ \exp\{\mathrm{ReTr}(M^{\dagger}U)\} \quad (3.4)$$

and

$$e^{\omega(\xi)} = \int (d\phi)\ \exp\{\mathrm{Re}(\xi^{\dagger}\phi)\} \quad , \quad (3.5)$$

then we have

$$Z = \int dV dM d\eta d\phi\ \exp\{-S_{eff}(V,M,\eta,\xi)\} \quad , \quad (3.6)$$

where the effective action is defined by

$$S_{eff}(V,M,\eta,\phi) = S(V,\eta) - \sum_{s,\hat{\mu}} [w(M_{s\hat{\mu}}) - \mathrm{ReTr}(M^{\dagger}_{s\hat{\mu}} V_{s\hat{\mu}})]$$

$$- \sum_{s} [\omega(\xi_s) - \mathrm{Re}(\xi^{\dagger}_s \eta_s)] \ . \qquad (3.7)$$

Saddle point conditions are obtained by differentiating S_{eff} by each unconstrained fields:

$$0 = \frac{\partial S_{eff}}{\partial M^{\dagger}_{ji}} = -\frac{\partial w}{\partial M^{\dagger}_{ji}} + \frac{1}{2} V^{ij} \ , \qquad (3.8a)$$

$$0 = \frac{\partial S_{eff}}{\partial \xi^{\dagger}_{i}} = -\frac{\partial \omega}{\partial \xi^{\dagger}_{i}} + \frac{1}{2} \eta^{i} \ , \qquad (3.8b)$$

$$0 = \frac{\partial S_{eff}}{\partial V^{\dagger}_{ji}} = \frac{\partial S}{\partial V^{\dagger}_{ji}} + \frac{1}{2} M^{ij} \ , \qquad (3.9a)$$

$$0 = \frac{\partial S_{eff}}{\partial \eta^{\dagger}_{i}} = \frac{\partial S}{\partial \eta^{\dagger}_{i}} + \frac{1}{2} \xi^{i} \ , \qquad (3.9b)$$

and their hermitian conjugates.

Substituting V^{ij} and η^{i} into Eqs.(3.9a,b) by use of Eqs. (3.8a,b), we obtain coupled equations for M^{ij} and ξ^{i}. We impose, as usual, the condition that solutions are invariant under translations. Further we assume that M^{ij} is proportional to a unit matrix, for convenience. This assumption is an unpleasant point of the present analysis, since with this assumption we are indifferent to the residual degrees of freedom which survive after the symmetry breakdown. The disadvantage of this assumption will be discussed in the next section. Thus we assume

$$M^{ij}_{s_{\hat{\mu}}} = m\ \delta^{ij} \tag{3.10a}$$

and

$$\xi^i_s = \xi\ n^i\ , \tag{3.10b}$$

where n^i is a complex three-dimensional unit vector, i.e., $\Sigma_i |n^i|^2=1$. Characteristic functions $w(M)$ and $\omega(\xi)$, and their derivatives are calculated so that (for details of calculations see appendix)

$$w(M)\Big|_{M=m\mathbb{1}} = w(m)$$

$$= \ln \sum_{n=-\infty}^{\infty} \det \begin{vmatrix} I_n(m) & I_{n-1}(m) & I_{n-2}(m) \\ I_{n+1}(m) & I_n(m) & I_{n-1}(m) \\ I_{n+2}(m) & I_{n+1}(m) & I_n(m) \end{vmatrix} \tag{3.11}$$

$$\frac{\partial w}{\partial M^{\dagger}_{ji}}\Bigg|_{M=m\mathbb{1}} = \frac{1}{6} w'(m)\delta^{ij}\ , \tag{3.12}$$

$$\omega(\xi)\Big|_{\xi^i=\xi n^i} = \omega(\xi) = \ln\left(\frac{8I_2(\xi)}{\xi^2}\right)\ , \tag{3.13}$$

$$\frac{\partial \omega}{\partial \xi^{\dagger}}\Bigg|_{\xi^i=\xi n^i} = \frac{1}{2}\omega'(\xi)n^i = \frac{I_3(\xi)}{2I_2(\xi)} n^i\ , \tag{3.14}$$

where $I_n(x)$ is a modified Bessel function of the n-th order. Substitution of these expressions leads to the following stationary conditions

$$4\beta^* w'(m)^3 + \gamma^* \omega'(\xi)^2 - m = 0 \quad , \tag{3.15}$$

$$8\gamma^* w'(m)\omega'(\xi) - \xi = 0 \quad , \tag{3.16}$$

where $\beta^* = \beta/54$ and $\gamma^* = \gamma/3$. The mean-field free energy density is written as

$$F_{MFA} = 4[\ \beta^* - \beta^* w'(m)^4 - w(m) + mw'(m) + \gamma^* - \gamma^* w'(m)\omega'(\xi)^2] - \omega(\xi) + \xi\omega'(\xi) \tag{3.17}$$

$$= 4\beta^* - 4w(m^*) + 3m^* w'(m^*) + 4\gamma^* - \omega(\xi^*) + \frac{5}{8}\xi^* \omega'(\xi^*) \quad , \tag{3.18}$$

where m^* and ξ^* are solutions of Eqs.(3.15) and (3.16).

For the case of the adjoint representation, the approximation is carried out in the same way. The characteristic function for a scalar field turns out to be

$$\omega_A(\xi)\Big|_{\xi^a = \xi n^a} = \omega_A(\xi) = \ln\left(\frac{48 I_3(\xi)}{\xi^3}\right) \quad . \tag{3.19}$$

The stationary conditions are

$$4\beta^{*}w'(m)^{3}+\frac{2}{3}\gamma^{*}w'(m)\omega_{A}'(\xi)^{2}-m=0 \tag{3.20}$$

and

$$\frac{8}{3}\gamma^{*}w'(m)^{2}\omega_{A}'(\xi)-\xi=0 \quad . \tag{3.21}$$

The free energy density is given by

$$\begin{aligned} F_{MFA} = 4[\ &\beta^{*}-\beta^{*}w'(m)^{4}-w(m)+mw'(m) \\ &+\gamma^{*}-\frac{\gamma^{*}}{3}w'(m)^{2}\omega'(\xi)^{2}]-\omega(\xi)+\xi\omega'(\xi) \end{aligned} \tag{3.22}$$

$$\begin{aligned} = \ &4\beta^{*}-4w(m^{*})+3m^{*}w'(m^{*}) \\ &+4\gamma^{*}-\ \omega(\xi^{*})+\frac{3}{4}\xi^{*}\omega'(\xi^{*}) \end{aligned} \tag{3.23}$$

§4 Results of numerical calculations

Before presenting results, it is helpful for us to see the property of first-derivatives of characteristic functions. We plot them in Fig.2. They approach to limiting values as the relevant parameters tend to infinity and their values are bounded in the ranges, $-3/2<w'(m)<3$ and $-1<\omega'(\xi)<1$. This behaviour reminds us that they are directly related to the mean fields V^{ij} and η^i through stationary conditions. For scalar fields they are odd functions of ξ, but $w'(m)$ is not because the measure for $Tr(U)$ is not symmetric under the change of a sign. All of them are increasing functions and their derivatives, i.e. the second derivatives of characteristic functions, are positive. Thus, the result is consistent with the negligence of $w''(m)$ and $\omega''(\xi)$ in the derivation of stationary conditions.

We have searched solutions for the stationary conditions (3.15,16) and (3.20,21) by numerical calculations in the region $0\leq\beta\leq 10$ and $0\leq\gamma\leq 15$. In both cases of the representation of the scalar fields, we have obtained three types of solutions:

(i) $\xi=m=0$

Equations (3.15) and (3.16), or (3.20) and (3.21) are trivially satisfied for any values of β and γ. All the mean fields vanish, showing both gauge and scalar fields are disordered (a confined phase). The free energy density receives a contribution only from constant terms:

$$F^{(i)}_{MFA} = 4\beta^{*}+4\gamma^{*} \quad . \tag{4.1}$$

For convenience, we redefine the free energy density by subtracting the above value in the following discussions. Therefore, F=0 for this solution.

(ii) $\xi=0$, $m\neq 0$

The condition (3.16) or (3.21) is satisfied trivially, and the other one reduces to that of the pure gauge system

$$4\beta^{*}w'(m)^{3}-m=0 \quad . \tag{4.2}$$

We show the behaviour of $w'(m)^{3}$ and $m/(4\beta^{*})$ for a typical value of β^{*} in Fig.3. Solutions are given by the values of m at crossing points of two curves. For β^{*} less than a certain critical value, there is no solution other than m=0, but for β^{*} large enough, there appear two positive solutions. The larger one corresponds to the minimum of the free energy. The β dependence of the solution m^{*} can be obtained by Eq.(4.2). If m is large enough, $w'(m)$ can be considered to be a constant. Then we have

$$m^{*}\cong 2\beta \quad . \tag{4.3}$$

The numerical solutions are shown in Fig.4(a) (a solid line). As expected, a solution appears in the weak coupling region $\beta\gtrsim 7$ and

m^* grows with along the line parallel to the line of (4.3) (a broken line). We note that this solution exists for any γ. The free energy density for the pure gauge system in the mean field approximation is given by

$$F_{MFA}^{(ii)} = -4w(m^*)+3m^*w'(m^*) \quad . \tag{4.4}$$

If we use (4.3), we have an approximate form

$$F_{MFA}^{(ii)} \cong -4w(2\beta)+18\beta \quad . \tag{4.5}$$

The resultant free energy density is plotted in Fig.4(b), where the approximate one is also shown (a broken line). The system undergoes a transition at the value of m where $F_{MFA}^{(ii)}(m^*)$ vanishes ($=F_{MFA}^{(i)}$). From Fig.4(b) the critical point is determined so that $\beta \cong 8$. Because the stationary point appears before the transition, it is the first order critical point. For the solution with $\xi=0$ we see that the spin configuration is disordered and hence we interprete the phase above the critical point as a deconfined symmetric phase. As described in the introduction, the non-existence of such a critical point has been verified by MCS. It is discussed by Flyvbjerg et al. for the SU(2) pure gauge system that the mean-field critical point which appears also in the SU(2) case is expected to vanish, if we take into account the higher-order effects. We expect that the mean-field critical point in the SU(3) case also vanishes.

In the case of extremely large values of β ($\beta \gtrsim 100$), there appears negative solutions. We have made a simplified analysis and found that it is a local minimum with a larger value of the free energy. So we will neglect it in the following discussions.

(iii) $\xi \neq 0$, $m \neq 0$

A solution of this type corresponds to the higgs phase. An existence of such a solution can be seen as follows. For large values of m and ξ, we can take $w'(m) \simeq 3$ and $\omega'(\xi) \simeq 1$ and the stationary condition gives

$$m^* \cong 2\beta + \frac{1}{3}\gamma \quad \text{(for the case of fundamental repr.)}\,, \qquad (4.6a)$$

$$m^* \cong 2\beta + \frac{2}{3}\gamma \quad \text{(for the case of adjoint repr.)} \qquad (4.6b)$$

and

$$\xi^* = 8\gamma \quad . \qquad (4.7)$$

According to the consistency with the large values of m and ξ one requires that this type of the solution appears in the region of large γ. Using above equations, the free energy density (3.18) and (3.23) become

$$F_{MFA}^{(iii)} \cong -4w(2\beta + \frac{1}{3}\gamma) - \omega(8\gamma) + 18\beta + 8\gamma \quad \text{(fund. repr.)} \qquad (4.8a)$$

and

$$F_{MFA}^{(iii)} \simeq -4w(2\beta+\frac{2}{3}\gamma)-\omega(8\gamma)+18\beta+12\gamma \quad \text{(adj. repr.)}. \qquad (4.8b)$$

Stereographical views of solutions m^* and ξ^*, and of the free energy (in the figure, -F is plotted for convenience) are given in Fig.5 for the case of the fundamental representation and in Fig.6 for the case of the adjoint one. In both cases, the solutions are obtained at the mesh points of solid lines. The dotted lines are drawn in order to display the position where the solutions exist. The broken lines are intersections of the above approximate forms with the boundaries. The Eqs. (4.6), (4.7) and (4.8) well reproduce the real solutions, in spite of such a simple estimation. A mesh of broken lines in the Fig.5(c) and Fig.6(c) shows that the free energy is positive there. For the sake of the later discussions, we plot the free energy of the type-(ii) solution in connection with the type-(iii) one (in the region near the pure gauge limit).

§5. Discussions of the results

Now we can draw phase diagrams based on the numerical results. The determination of the phase is carried out by examining the behaviour of the free energy. We have to choose a solution with a minimum free energy density (maximum for -F).

First we discuss the system with a scalar field belonging to the fundamental representaion. In Fig. 5(c) we have plotted -F for the type-(iii) solution. The free energy density for the type-(ii) solution is also plotted in the region $\gamma<1$. It may, however, be extended to the region of larger values of γ, since the type-(ii) solution does not depend on γ. The free energy for the type-(i) solution vanishes for any values of parameters and it is represented by a -F=0 plane in Fig. 5(c). It is easy to see that there are three phases corresponding to the three solutions.

(I)	confined phase	for small values of β and γ
(II)	deconfined symmetric phase	for $\beta\geqq8$, and $\gamma\lesssim1$
(III)	higgs phase	for the remaining part

Let us discuss the property of phase boundaries. As described in §4, the boundary between (I) and (II) is expected to vanish for the SU(3) pure guage system, if we incorporate the higher-order corrections. In the present model, there is additional contributions from the scalar field. Studies of this contribution to the higher-order corrections are an interesting problem, but here we consider naively that it does not change the situation since γ is small in the relevant region. Thus we expect that the phase boundary between (I) and (II) is not a true transition line and that the confined phase is smoothly connected to the deconfined symmetric one.

The boundary between (II) and (III) runs along $\gamma=1$ in the weak coupling region ($\beta\gtrsim 8$). The free energy for the type-(III) solution seems to be smoothly connected to that of the type-(II) one. The γ-dependense of the solution ξ^* verifies this fact. It decreases linearly with and vanishes at around $\gamma=0.5$, i.e. it coincides with the type-(II) solution. All of these behaviours point to the suggestion that this line is of the second order. We have made a further analysis on this point. We have calculated the free energy (3.17) as a function of ξ by fixing m to m^*. Note that it may be considered as an effective potential for the scalar field. In Fig. 7, we exhibit the shape of the free energy for typical values of γ (at $\beta=10$). The variation of the shape clearly shows that this transition is of the second order.

The line separating (I) and (III) is of the first order in the region $\beta\gtrsim 3$, since the local minimum of the type-(iii) solution appears when the system lies still in the confined phase. In the strong coupling region $\beta\lesssim 3$, however, the surface representing $F_{MFA}^{(iii)}$ seems to be tangent to the F=0 plane. The solution appears as a global minimum. This fact suggests that the line of this region is of the second order. Since the transition is not caused solely by the scalar field, the analysis similar to that of Fig. 7 is ineffective. As described above, however, in the strong coupling limit no transition is expected. Therefore, we consider that it is actually of the second order and that this weakness indicates that the true transition line terminates before reaching the $\beta=0$ line.

Thus we obtain the phase diagram shown in Fig. 8. The solid (broken) line represents the first-order (second-order) transition and the dotted line at $\beta\simeq 8$ is considered to be a false one due to the inaccuracy of the lowest-order mean field approximation. If we add an end point to the transition line in the strong coupling region, the phase diagram looks the same as that of the Monte Carlo result (Fig. 1).

Next we consider the case of the scalar field in the adjoint representation. The behaviour of the free energy density Fig. 6(c) is very similar to that of Fig. 5(c). The difference is that the boundary between (I) and (III) is always of the first order. As mentioned in §3, there is a possibility that an Ising-like transition exists in the strong coupling limit. So there is no reason that the transition is weakened in this region in contrast with the above case. Thus we obtain the phase diagram as shown in Fig. 9.

The comparison with the Monte Carlo results[6] (Fig. 10) reveals a shortcoming of the mean field approximation supplemented by the assumption of $M^{ij}=m\delta^{ij}$. Monte Carlo simulations have shown that the parameter plane is divided into three parts at zero temperature: the SU(3)-confined phase, the SU(2)×U(1)-confined phase, and SU(2)-confined but U(1)-deconfined (higgs) phase. The last two are separated by the line starting from the U(1)-transition and run into the SU(3) broken phase ($\gamma>5$). It should be reminded that the region of large values of γ is governed by the type-(iii) solution in the whole range of β for the mean field results. The non-existence of the critical structure is regarded as a consequence of the assumption (3.10a). Because we have neglected the degrees of freedom surviving the SU(3)-breaking transition, it is natural that it cannot predict the transition caused by the U(1) gauge field. If we are to obtain such a transition, we have to use a mean field which can describe a detailed structure of the gauge fields.

Thus we conclude that the lowest order mean field approximation with the assumption (3.10a) predicts the phase diagram qualitatively consistent with Monte Carlo result in the case of the triplet scalar field, but, in the case of the octet scalar fields, it fails to give a transition caused by the gauge field of the residual symmetry of the spontaneously broken phase.

§6. Concluding remarks

We have studied the SU(3) lattice gauge system coupled with a scalar field on the basis of the mean field method. The lowest-order approximation gives a qualitatively good phase diagram in the case that the scalar field belongs to the fundamental representation. In the case of the scalar field in the adjoint representation, the resulting phase diagram is far from the expected one according to the fact that the assumed form of the mean gauge field is too simple. In order to improve the situation, we have to keep the residual degrees of freedom. One possibility is to permit diagonal elements of the mean field matrix to have different values. In that case the formulation resembles the analysis of the U(1) gauge system. The characteristic function for guage fields becomes, however, rather complicated and it is difficult to solve the self-consistency equations. Nevertheless investigations in this direction are needed to obtain the true phase structure.

The critical point predicted by MFA for the pure gauge system is expected to disapper by introducing the higher-order effects. How about the critical line in the strong coupling region? For the triplet scalar field it should terminate before reaching the $\beta=0$ limit, while for the octet one the critical structure is expected not to disappear. Can the higher-order analysis explain this difference? This is also an interesting problem to be studied.

Finally we comment on the finite temperature structure. The mean field method in the form developed in §3 has no information on the size of the lattice, since the assumption of translational invariance makes the free energy independent of it. The author have studied the system by admitting the time-component of gauge fields to have a different value, but the result obtained up to now has been always isotropic. If we take the different lattice spacing in the direction of time, it is possible to take the unisotropy into consideration. This method seems to be useful for the comparison with the Monte Carlo results of the finite temperature system. The conclusive statement is left for the future investigations.

Acknowledgement

The author expresses his cordial thanks to Professor T.Muta and Professor M.Kikugawa for valuable discussions. He is also grateful to Professor M.Yonezawa for encouragements.

Appendix

Here we show the detailed calculation of characteristic functions. First we derive that of the gauge field, $w(M^{ij})$, which is defined by

$$e^{w(M)} = \int (dU)\ e^{\mathrm{ReTr}(M^\dagger U)} \quad . \tag{A.1}$$

Since we assume that M^{ij} is proportional to a unit matrix δ^{ij} with a proportionality constant m, it is written as

$$e^{w(m)} = e^{w(M)}\Big|_{M=m1} = \int (dU)\ e^{m\mathrm{ReTr}(U)} \quad . \tag{A.2}$$

We express it as an integral of the diagonal elements,

$$e^{w(m)} = \int \frac{d^3\theta_i}{(2\pi)^3}\{1-\cos(\theta_1-\theta_2)\}\{1-\cos(\theta_2-\theta_3)\}\{1-\cos(\theta_3-\theta_1)\}$$
$$\times\delta(\Sigma\theta_i)_{\mathrm{mod}\ 2\pi}\ \exp(m\Sigma\cos\theta_i) \tag{A.3}$$

It reduces to the sum of four integrals

$$e^{w(m)} = \tfrac{3}{4}I_0-\tfrac{3}{2}I_1-\tfrac{3}{4}I_2+\tfrac{3}{2}I_3 \quad , \tag{A.4}$$

$$I_0 = \int d^3\theta_i\ \delta(\Sigma\theta_i)\ \exp\{m\Sigma\cos\theta_i\} \quad , \tag{A.5a}$$

$$I_1 = \int d^3\theta_i\ \delta(\Sigma\theta_i)\ \exp\{m\Sigma\cos\theta_i\}\ \cos(\theta_1-\theta_2) \quad , \tag{A.5b}$$

$$I_2 = \int d^3\theta_i \ \delta(\Sigma\theta_i) \ \exp\{m\Sigma\cos\theta_i\} \ \cos(2\theta_1 - 2\theta_2) \ , \quad (A.5c)$$

$$I_3 = \int d^3\theta_i \ \delta(\Sigma\theta_i) \ \exp\{m\Sigma\cos\theta_i\} \ \cos(3\theta_1) \ . \quad (A.5d)$$

Using an integral form of the modified Bessel function

$$I_n(m) = \frac{1}{2\pi}\int_{-\pi}^{\pi} d\theta \ e^{in \ +m\cos\theta} \ , \quad (A.6)$$

we obtain

$$e^{w(m)} = \sum_n \{I_n^3 - 2I_{n-1}I_nI_{n+1} - I_{n-2}I_nI_{n+2} + I_n^2(I_{n+3} + I_{n-3})\}. \quad (A.7)$$

We have not found an analytic form of this infinite sum. In practical calculation, we have added the number of terms as many as is necessary by using a computer.

The derivative of w(M) is given by

$$\left.\frac{\partial w}{\partial M^{\dagger}_{ji}}\right|_{M=m1} = \frac{1}{6}w'(m)\,\delta^{ij} \ , \quad (A.8)$$

where the facter 1/6 is obtained by comparing traces of both sides. Differenciating Eq.(A.7), we obtain

$$w'(m) = e^{-w} \sum_n \{I_n^2[I_{n+1} - I_{n+2} + I_{n+4} \quad (A.9)$$
$$-I_n[I_{n+3}I_{n1} - I_{n+4}I_{n+1} + I_{n+5}I_{n+2}]\}$$

Next we calculate the characteristic functions for scalar fields. Here we consider the scalar fields as real N-dimensional vectors. For the fundamental representation we take N=6 and for the adjoint one, N=8. The characteristic function is defined by

$$e^{\omega(\xi)} = \int d^N\vec{\phi}\ \delta(|\vec{\phi}|^2-1)\ e^{\vec{\xi}\cdot\vec{\phi}} \tag{A.10}$$

Replacing the delta function by its integral form we have

$$\begin{aligned} e^{\omega(\xi)} &\cong \int ds d^N\vec{\phi}\ e^{-s(\vec{\phi}\cdot\vec{\phi}\ -1)+\vec{\xi}\cdot\vec{\phi}} \\ &\cong \int ds\ s^{-\frac{N}{2}} e^{-s-\frac{\xi^2}{4s}}\ . \end{aligned} \tag{A.11}$$

Taking into account the normalization, we obtain

$$\omega(\xi) = \ell n\left(2^{\nu}\ \nu!\ \frac{I_{\nu}(\xi)}{\xi^{\nu}}\right) \tag{A.12}$$

where $\nu=N/2-1$. The derivative is given by

$$\omega'(\xi) = \frac{I_{\nu+1}(\xi)}{I_{\nu}(\xi)} \tag{A.13}$$

References

1) M.Creutz, Phys. Rev. Letters, **45** (1980), 313.
M.Creutz and K.J.M.Moriarty, Phys. Rev. **D26** (1982), 2166.

2) A.M.Polyakov, Phys. Letters **72B** (1978), 477.
L.Susskind, Phys. Rev. **D20** (1979), 2610.

3) T.Celik, J.Engels and H.Satz, Phys. Letters **125B** (1983), 411; Phys. Letters **129B** (1983), 323.
J.Kogut, M.Stone, H.W.Wyld, W.R.Gibbs, J.Shigemitsu, S.H.Shenker and D.K.Sinclair, Phys. Rev. Letters **50** (1983), 393.

4) A.H.Guth, Phys. Rev. **D23** (1981), 347.

5) M.Kikugawa, T.Maehara, T.Minazuki, J.Saito and H.Tanaka, Prog. Theor. Phys. **69** (1983), 1207.

6) M.Kikugawa, T.Maehara, J.Saito, H.Tanaka, Y.Yamaoka and R.Sasaki, Hiroshima Univ. preprint HUPD-8501 (1985).

7) E.Brezin and J.M.Drouffe, Nucl. Phys. **B200[FS4]** (1982), 93. See also J.M.Drouffe and J.B.Zuber, Phys. Report **102** (1983), 1.

8) B.J.Pendleton, Phys. Letters **118B** (1982), 121.

9) H.Flyvbjerg, B.Lautrup and J.B.Zuber, Phys. Letters **110B** (1982), 279.

10) J.Frohlich, B.Simon and T.Spencer, Commun. Math. Phys. **50** (1976), 79.

Figure captions

Fig.1: The phase diagram for the system with a scalar field (a) in the fundamental representation and (b) in the adjoint representation obtained by Monte Carlo simulations, taken from Ref.5) and 6), respectively.

Fig.2: The first derivatives of characteristic functions for (a) the gauge variable, (b) the scalar field in the fundamental representation and (c) the scalar field in the adjoint representation.

Fig.3: The first derivative of the characteristic function cubed for the gauge variable as a function of m. Solutions of the saddle-point equation for the pure gauge system are given as a function of m at the points crossing with a line $m/(4\beta^*)$, which is shown for a typical value of β^*.

Fig.4: (a) A solution m^* of the stationary condition for the pure gauge system as a function of β. The broken line represents the approximate solution of Eq.(4.3). (b) The free energy density corresponding to the solution, also, as a function of β. The broken line is again the free energy density estimated by the approximate solution.

Fig.5: Stereographical view of solutions for (a) m and (b) ξ of the type (iii), and (c) the corresponding free energy density, in the case of the system with a triplet scalar field. Dotted lines show the positions where the solutions appear. Broken lines are intersections of the approximate solutions and boundaries. In (c), a broken mesh represents that the free energy is positive there.

Fig.6: Stereographical view of solutions for (a) m and (b) ξ of the type (iii), and (c) the corresponding free energy density, in the case of the system with an octet scalar field. The differences of line types are same as Fig. 5.

Fig.7: The free energy $F_{MFA}(m=m^*)$ at $\beta=10$ as a function of ξ for three values of γ.

Fig.8: Phase diagram obtained by MFA for the case of the scalar field in the fundamental representation. A solid (broken) line is considered to be of the first (second) order. The dotted line is expected to disappear if we take into account higher-order effects.

Fig.9: Phase diagram obtained by MFA for the case of the scalar field in the adjoint representation.

Fig.10: Phase diagram at zero temperature obtained by Monte Carlo simulations for the case of the scalar field in the adjoint representation, taken from Ref. 6).

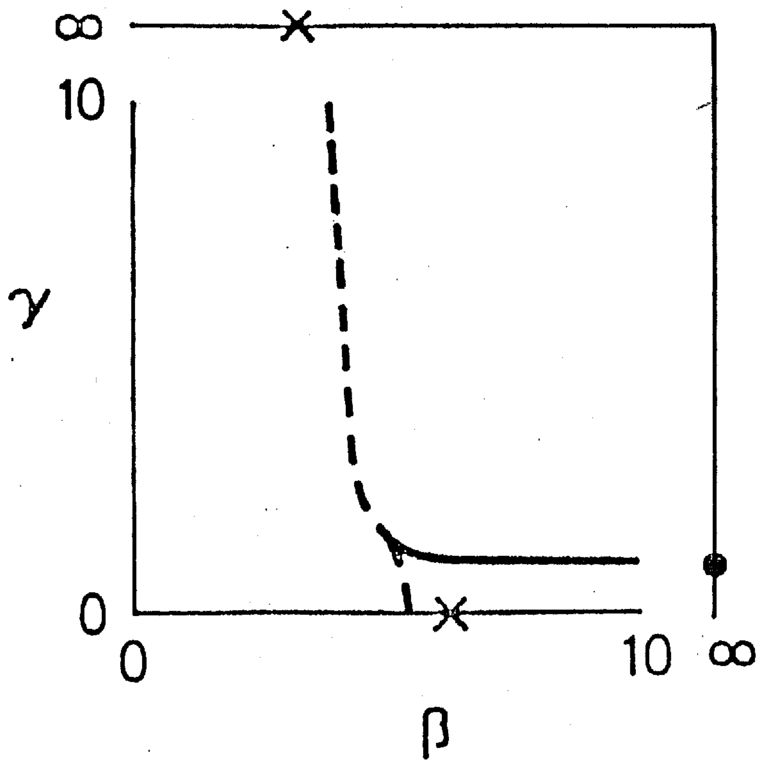

(a)

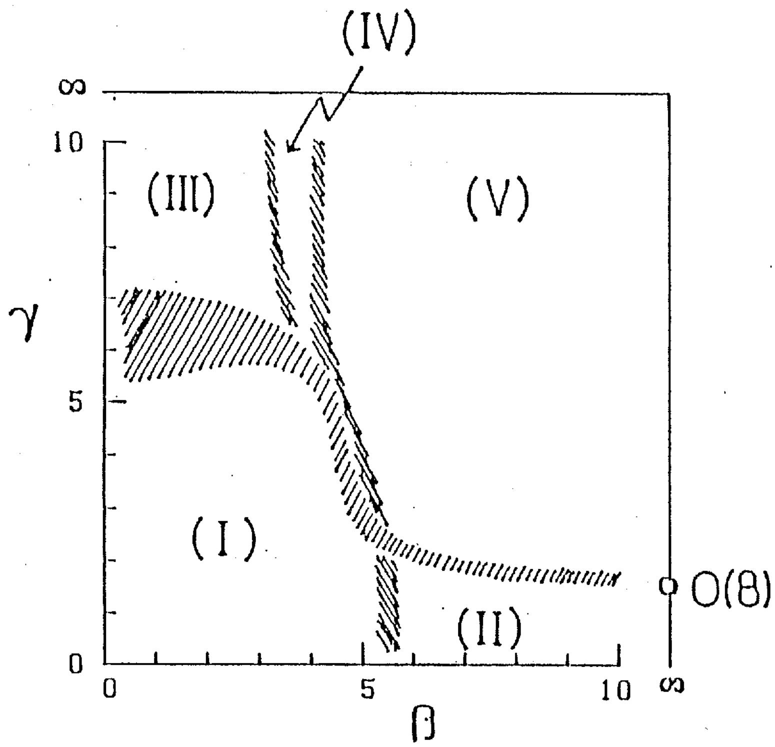

(b)

Fig. 1

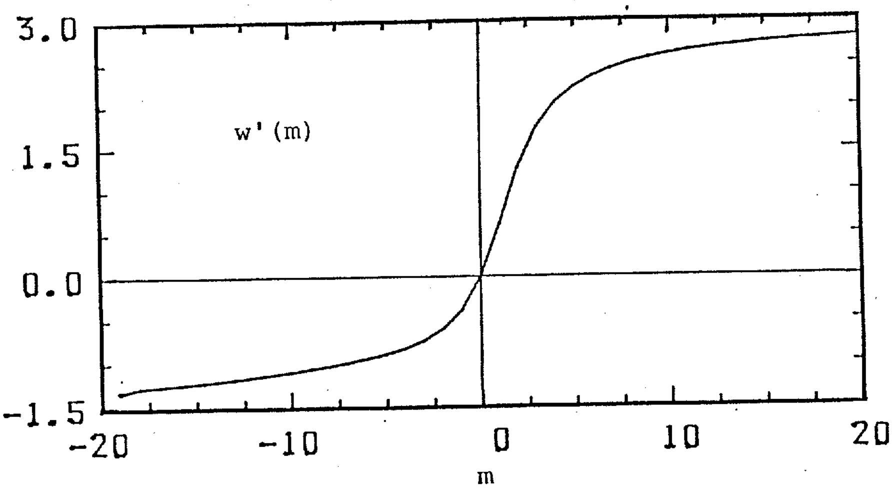
3.0
1.5
0.0
-1.5
w'(m)
-20
-10
0
10
20
m

(a)

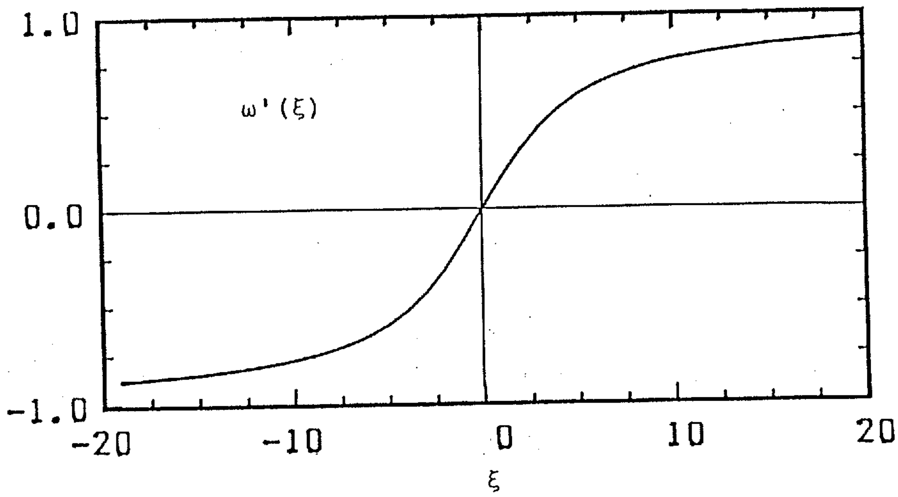
1.0
0.0
-1.0
ω'(ξ)
-20
-10
0
10
20
ξ

(b)

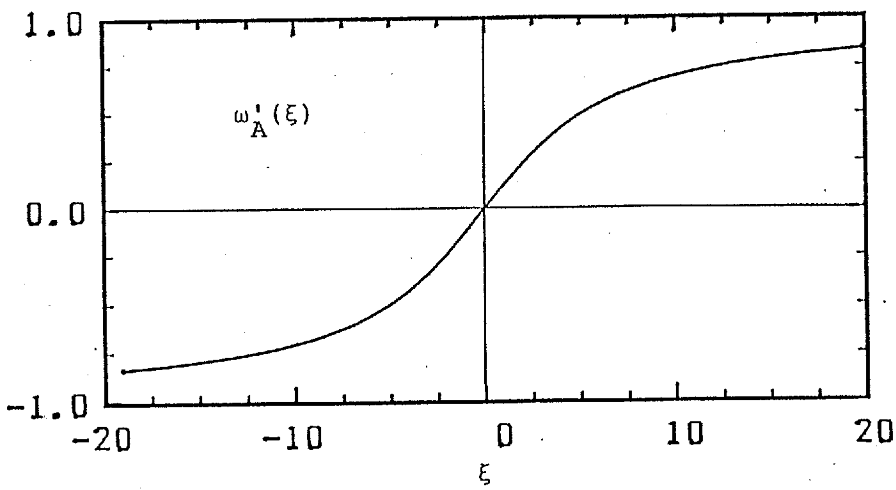
1.0
0.0
-1.0
ω'A(ξ)
-20
-10
0
10
20
ξ

(c)

Fig. 2

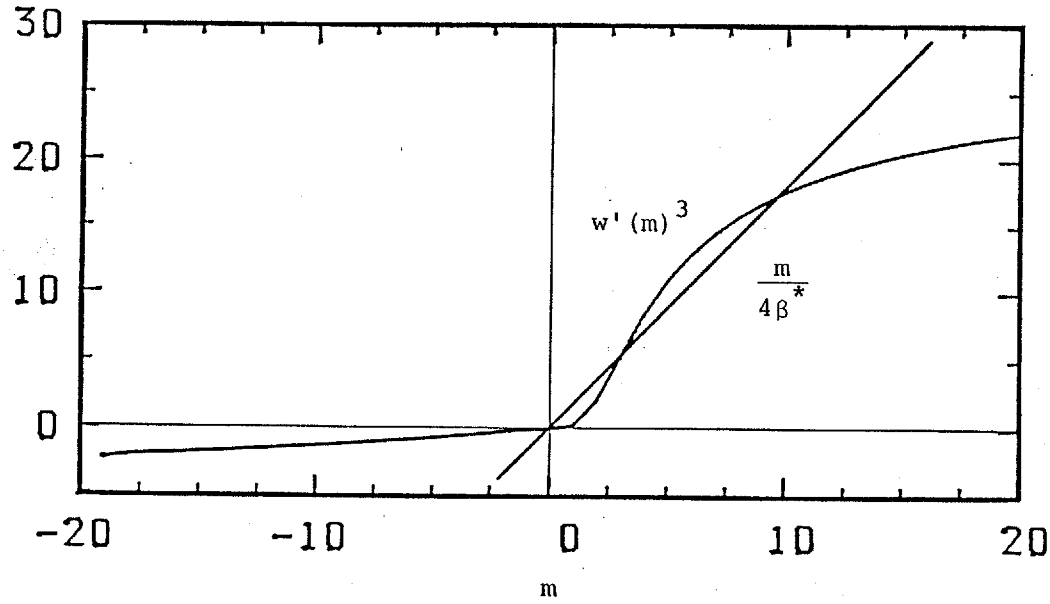

Fig. 3

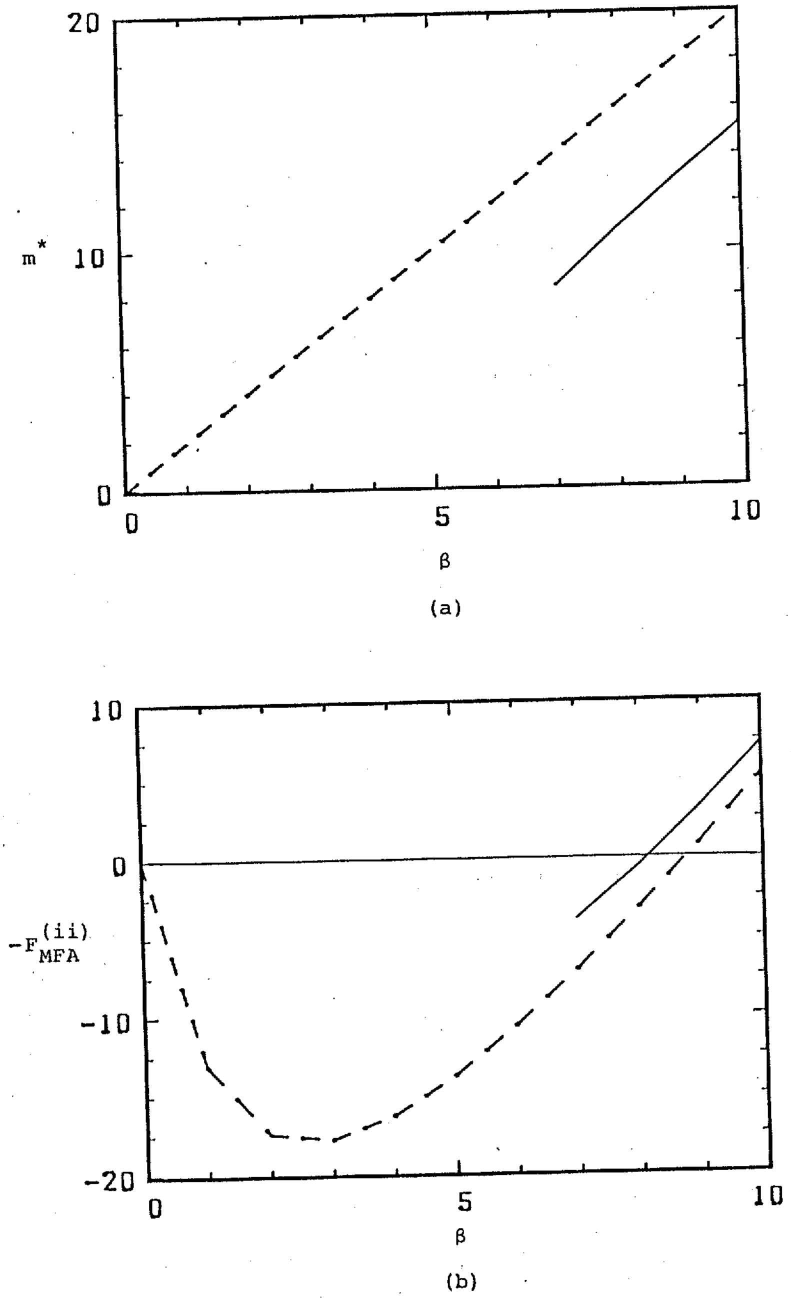

<u>Fig. 4</u>

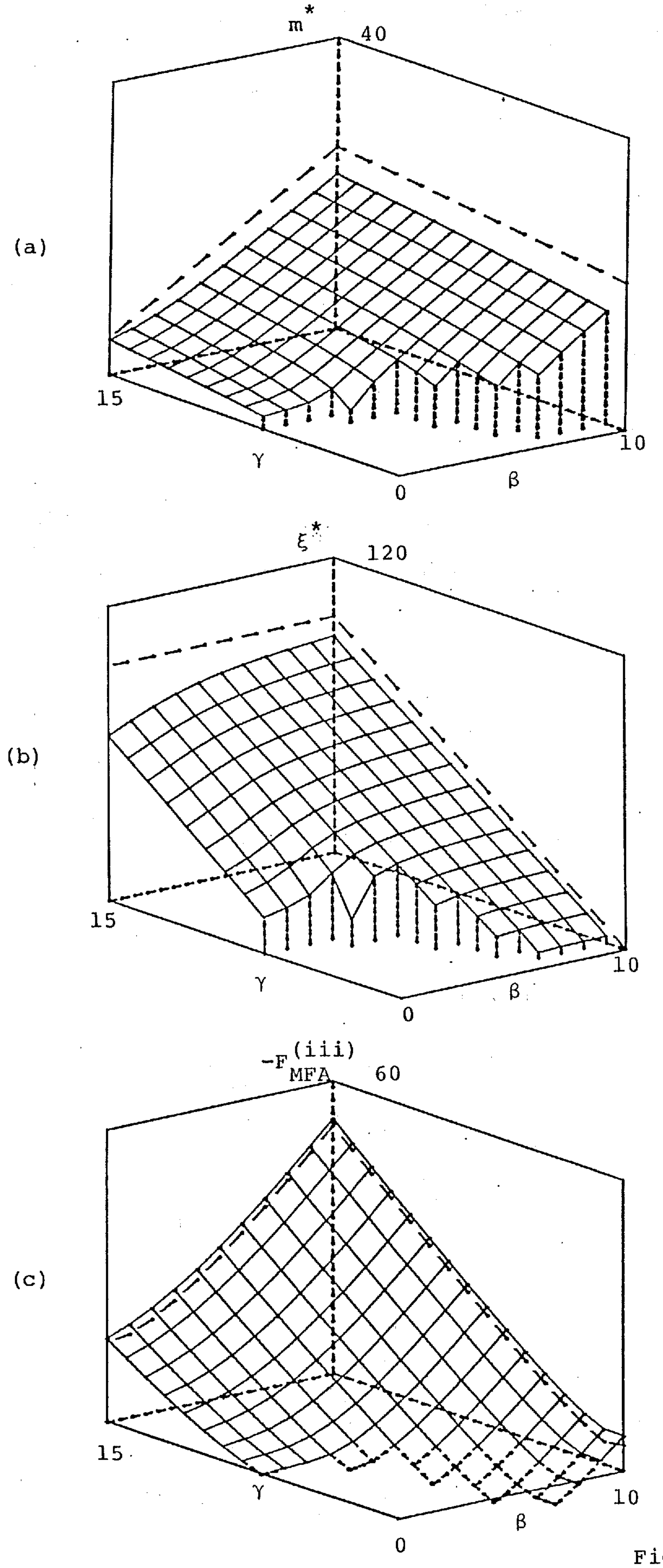

Fig. 5

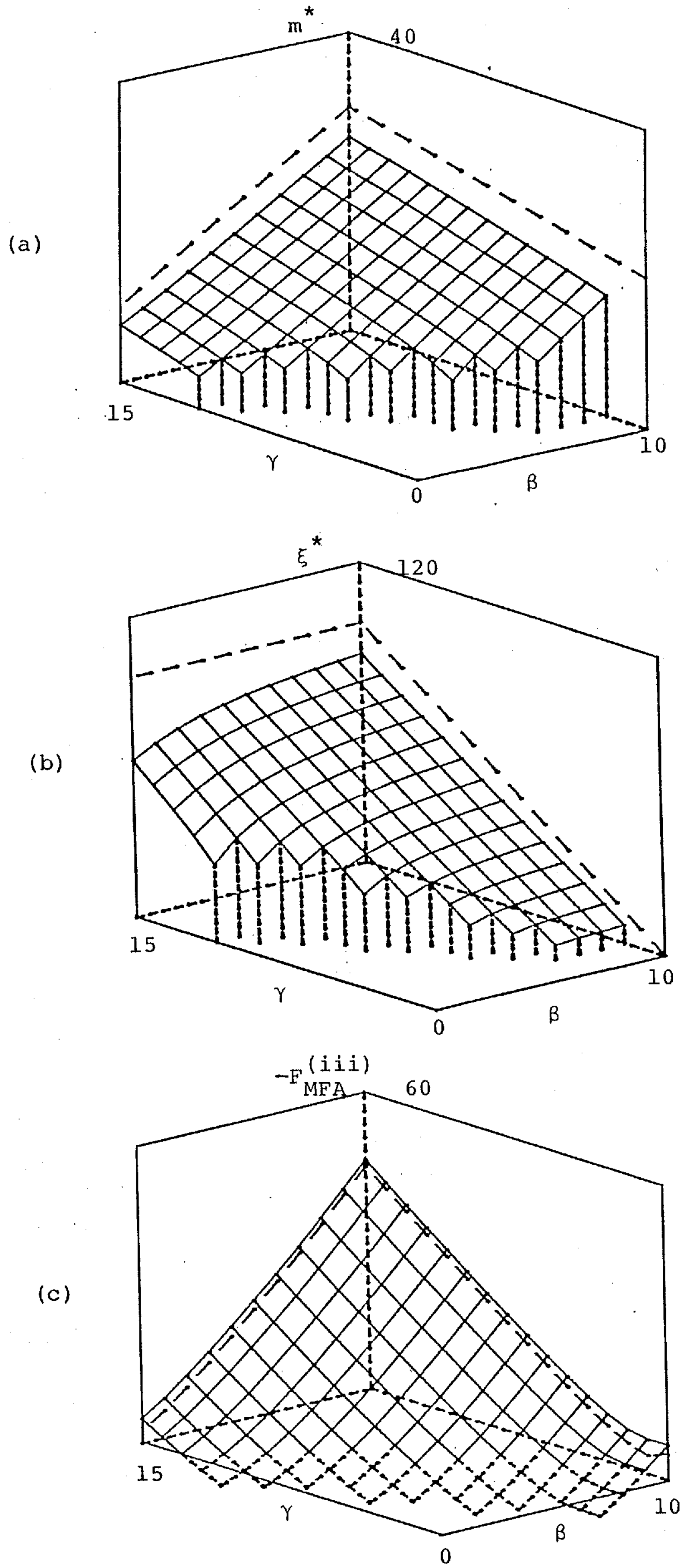

Fig. 6

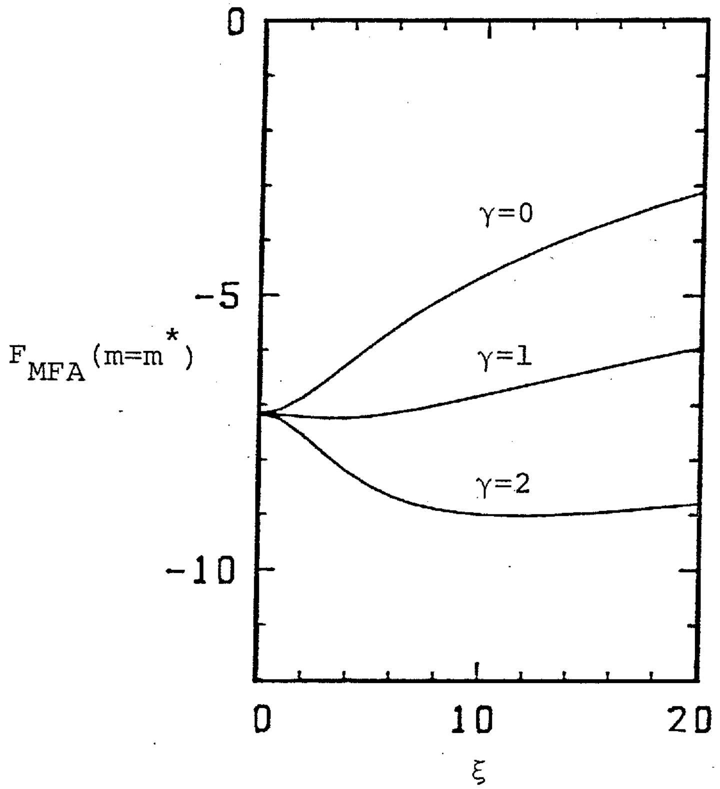

Fig. 7

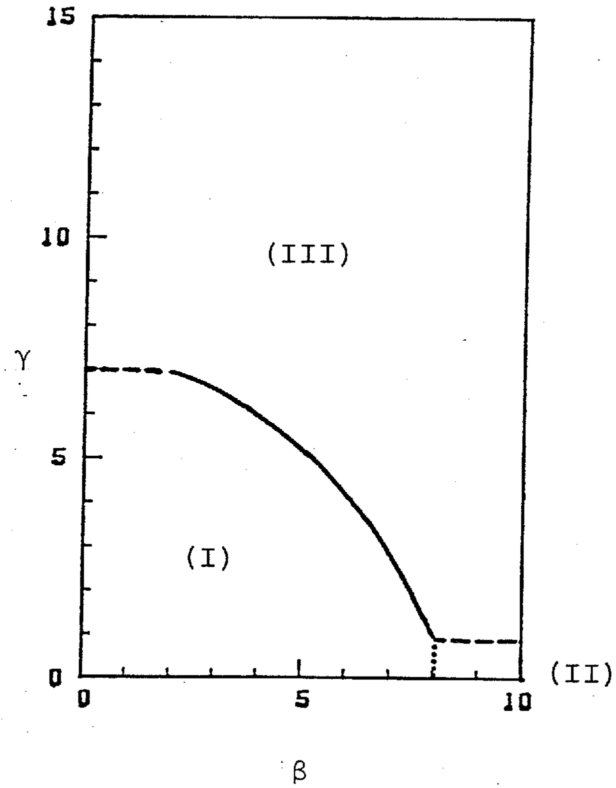

Fig. 8

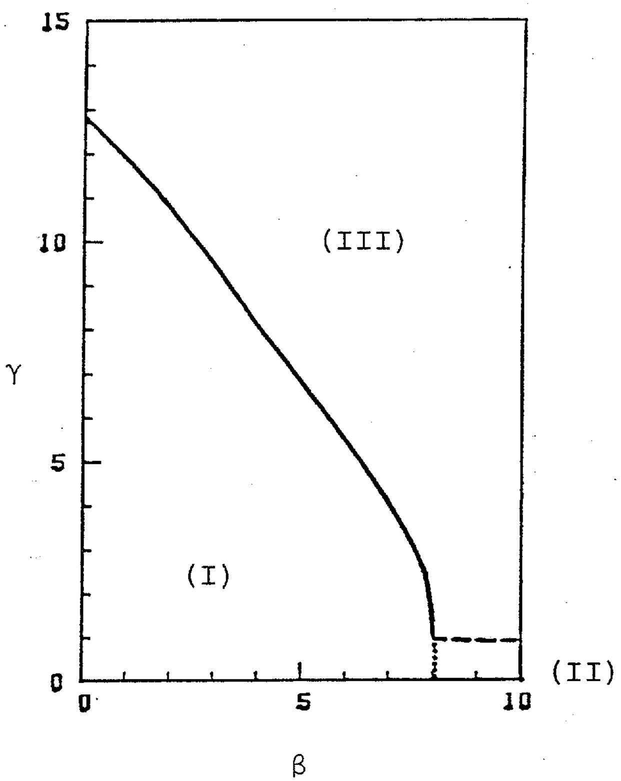

Fig. 9

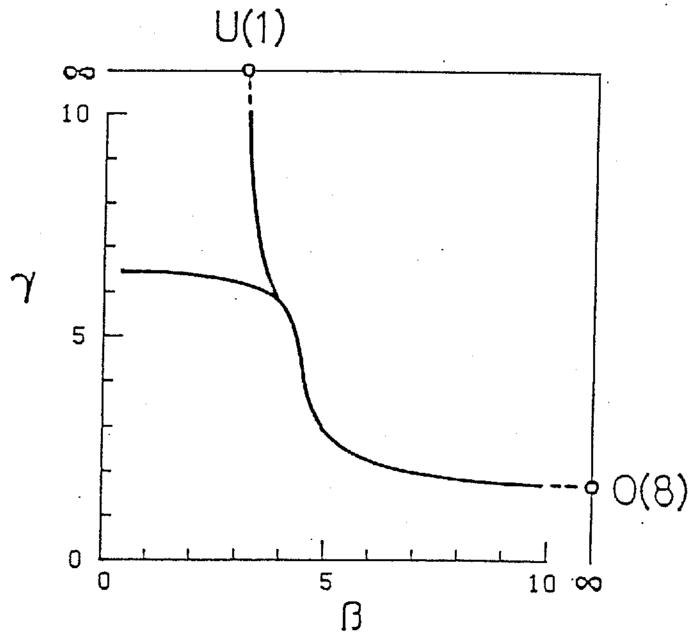

Fig. 10